Vibrationally resolved photoelectron angular distributions and branching ratios for the carbon dioxide molecule in the wavelength region 685–795 Å

J. B. West, M. A. Hayes, and M. R. F. Siggel
Daresbury Laboratory, Warrington WA4 4AD, United Kingdom

J. L. Dehmer and P. M. Dehmer
Argonne National Laboratory, Argonne, Illinois

A. C. Parr and J. E. Hardis
National Institute of Standards and Technology, Gaithersburg, Maryland 20899

(Received 14 November 1995; accepted 13 December 1995)

Measurements of vibrational branching ratios and photoelectron angular distributions have been made in the regions of the Tanaka-Ogawa, Lindholm, and Henning series for the CO_2 molecule. The behavior of these parameters was found to be sensitive to which particular resonance is excited, with considerable intensity going into vibrational modes other than the symmetric stretch. An initial analysis of some of the data taken is presented. © *1996 American Institute of Physics.* [S0021-9606(96)01311-0]

I. INTRODUCTION

It has been known for some time that the photoionization spectrum of carbon dioxide contains prominent series of autoionizing resonances converging to the $A\ ^2\Pi_u$ and $B\ ^2\Sigma_u^+$ ionization limits. Although not all the structure has been identified, several vibrational and Rydberg progressions have been designated as the Tanaka–Ogawa (TO) series, the Lindholm (L) series and the Henning sharp (s) and diffuse (d) series. Using spectrographic methods, Tanaka and Ogawa[1] identified several Rydberg series converging onto the first eight vibrational levels of the A state. Each of these levels is split by spin–orbit coupling, with the series converging onto the $^2\Pi_{1/2}$ limit being the stronger. A further progression seen by Tanaka *et al.*[2] was later assigned by Lindholm[3] as a vibrational progression with principal quantum number 3. The other most prominent series were first seen by Henning[4] and converge to the ground vibrational level of the B state of the CO_2^+ ion; Tanaka and Ogawa also found a Rydberg series converging to the first vibrational level of the B state. McCulloh[5] carried out a photoionization mass spectrometry experiment and tabulated all the above series, incorporating the quantum defect analysis of Lindholm[3] and using a notation which we have followed in this work. A full consideration of the symmetries of the series was given recently by Parr *et al.*[6] In summary, in the case of the TO series some doubt remains but theoretical[7,8] evidence points to the TO series having an $nd\delta_g$ configuration; on the other hand, the Henning sharp and diffuse series are now firmly believed to have $nd\sigma_g$ and $ns\sigma_g$ symmetries, respectively. The Lindholm series, called an ''additional progression'' by Tanaka *et al.*,[2] was tentatively assigned by Lindholm[3] to be a Rydberg series with nd symmetry converging to the A state of the ion.

The study presented here was undertaken to examine the response of angular distribution parameters and branching ratios to complex resonant structure in the photoionization spectrum. Our measurements were made with improved electron spectrometer resolution and a wider wavelength range than the earlier study by Holland *et al.*[9] in which the branching ratios were measured. The electron resolution requirement was important because it is well known (see, for example, the measurements on CO_2 by Parr *et al.*[10]) that both bending and antisymmetric stretch modes are populated in resonant regions as a result of vibronic interaction. In order to obtain reliable intensities for these bending and stretching levels, an electron spectrometer resolution of much better than the 156.7 meV energy spacing of the symmetric stretch frequency was required. Both these requirements were met by the combination of an electron spectrometer system comprising two hemispherical analyzers, and a 5 m normal incidence spectrometer. Having provided the first measurements of this kind, vibrationally resolved angular distributions on a triatomic molecule, the further aim was to examine again the evidence for the assignments of the autoionizing series, particularly the TO and L series where some uncertainty still remains.

II. EXPERIMENTAL PROCEDURE

This experiment was carried out on the 5 m normal incidence monochromator[11] fitted to a beamline at the Daresbury SRS, providing a photon flux of $\sim 10^{10}$ photon/s within a bandpass of 0.1 Å. The light was brought into the experimental chamber by a 2 mm diameter capillary light guide, which also served as a pressure differential between this chamber and the ultrahigh vacuum of the optical monochromator. The electron spectrometer, comprised of two 100 mm radius hemispherical analyzers, one rotatable about the incoming light beam as an axis of rotation and the other fixed, was contained in a chamber shielded from magnetic fields by three layers of μ metal. The fixed analyzer accepted electrons ejected parallel to the E vector of the incident radiation,

and after calibration procedures were completed the rotatable analyzer was set perpendicular to the E vector.

Calibration of the energy response of the analyzers was done using argon and helium gases, using the known values of the cross section[13] and β parameters[14] and following standard procedures.[15] The electron spectrometer resolution was determined from the rare gas calibration to be about 41 meV for the fixed analyzer and 46 meV for the rotatable analyzer, for all the rare gas spectra taken. The optical monochromator resolution was 0.1 Å (~2 meV) for the measurements taken at wavelengths shorter than 750 Å. At wavelengths longer than this, where the structure in the absorption spectrum is less dense, the wavelength resolution was 0.2 Å.

The polarization of the incoming light was measured using a three mirror polarizer with tungsten mesh and plate photodiodes, which could be rotated with the rotatable analyzer. The polarization needed to be checked frequently since small movements in the storage ring beam position and the mirrors focusing the light onto the entrance slit of the monochromator can have a marked effect on the polarization. It was found that, provided the premirror adjustments were kept optimized for maximum photon flux from the exit slit of the monochromator, the polarization remained stable. Full details of this instrument have been published by Parr *et al.*,[12] the main difference from the description there being the incorporation of multichannel detectors in the exit planes of the analyzers.

Throughout the whole wavelength region studied here, measurements were taken at 0.1 Å intervals. The expression for the differential cross section giving the angular distribution in the plane normal to the photon propagation direction is

$$\frac{d\sigma}{d\Omega} = \frac{\sigma}{4\pi}\left[1+(\beta/4)(3p\,\cos 2\theta+1)\right],$$

where θ is the angle between the major polarization axis and the ejected electron, Ω is the solid angle of collected electrons, p is the polarization of the incoming light, and σ is the partial cross section for the channel corresponding to the photoelectron being detected. The β parameters and branching ratios were calculated from the measurements made at the two angles $\theta=0°$ and $\theta=90°$.[16] We define the vibrational branching ratio as follows: The intensity going into a particular vibrational level of the ground state of the ion divided by the sum of the intensities of all the measured vibrational levels. The number of electrons detected within the constant solid angle of acceptance of the detection system and for an integrated photon flux is proportional to the differential cross section. Hence by measuring the number of electrons at two angles, $\theta=0°$ and $\theta=90°$ are used, for a given integrated photon flux, the parameter β can be determined along with a number which is proportional to the partial cross section for the process. Specifically the ratio of the signals at $\theta=0°$ and $\theta=90°$ allow for the determination of β. The number of electrons per solid angle for the given photon flux calculated for the value of θ_m where $3p\cos 2\theta_m=-1$, is the number proportional to the total cross section for the process. The angle, θ_m, is an effective ''magic angle'' for this technique. These calculated numbers can be used to evaluate the relative partial cross sections or branching ratios for the various processes leaving the CO_2^+ ion in differing final states.

III. DATA ANALYSIS

The analysis of this large amount of data required careful organization and a reliable method of extracting the highly detailed information which it contained. The first stage was to correct the raw data for the differing detection efficiencies of the two electron energy analyzers. This correction is a function of the kinetic energy of the electron, and was determined by analysis of the angular distribution data from the rare gases. Upon normalization for detection efficiencies, the data were fitted to a series of gaussian profiles using a least squares procedure.

The $^2\Pi$ ground state of CO_2^+ is spin–orbit split into two components approximately 19 meV apart, and furthermore the bending mode populated in resonance regions is also split by a similar amount due to Renner–Teller coupling. We did not attempt to resolve these splittings in the present experiment, and the effect was manifest as an apparent broadening of the photoelectron peaks in CO_2^+ compared to the rare gases. An effective peak width for CO_2^+ data was calculated by fitting a single Gaussian to two Gaussian peaks of the width determined by the rare gases but displaced by the 19 meV splitting. Some slight adjustments to obtain minimal error in the fitting gave effective values of 46 and 56 meV for the effective resolutions of the two analyzers. Since the spectra were unresolved and consisted of peaks in the model that were closer than the experimental resolution, it became necessary and prudent to fix the peak width parameter in the least squares fitting routine in order to obtain fits that made physical sense. Since the resolution of the analyzers was constant as determined by the rare gas calibrations, this constraint is reasonable and permits the data to be analyzed in a uniform manner.

The spectroscopic values of the vibrational parameters, using a combination of the literature[17,18] values and best fits to our data, were found to be $\omega_1=156.7$ meV, $\omega_2=60.0$ meV, and $\omega_3=182.3$ meV. These values gave good fits to the data over a broad range of electron kinetic energies and represent an averaging over the levels split by the spin–orbit and Renner–Teller interactions. The transitions to the asymmetric stretch ω_3 and bending mode ω_2 with odd numbers of quanta are forbidden from the ground state but have been observed in other photoelectron work reported in the literature.[19] Though contrary to the Franck–Condon principle, this is now a well established phenomenon in resonance regions and can be ascribed to anisotropic interactions of the escaping electron with the molecular core, leading in turn to a violation of the selection rules. The presence of these transitions and the Renner–Teller splitting of the bending modes give rise to an overlap of the possible transitions, and this makes a unique identification of the photoelectron peaks we observed impossible except in some prominent circumstances. Chambaud *et al.*[20] have identified many of the low lying vibrational levels of CO_2^+ which can be used as a

basis for estimating the positions and compositions of the levels we observe. Using the notation (v_1,v_2,v_3), where v_1 is the quantum number of the symmetric stretch, v_2 the quantum number of the bending mode, and v_3 that of the asymmetric stretch, we find the spectra can be accounted for adequately by the following set of transitions:

$$(v_1,0,0), \quad v_1 \geqslant 0,$$

$$(v_1,1,0), \quad v_1 \geqslant 0,$$

$$(v_1,2,0), \quad 0 \leqslant v_1 \leqslant 4,$$

$$(v_1,0,1), \quad 0 \leqslant v_1 \leqslant 5,$$

$$(v_1,1,2), \quad v_1 \geqslant 3.$$

The upper value of v_1 is determined by the span of the energy range covered by the photoelectron spectra. In some cases it was not necessary to include the $(v_1,0,1)$ or $(v_1,1,2)$ levels, as the intensity in the high binding energy region was small and the structure was adequately represented by the simpler set of levels.

It is possible other types of excitations may contribute to the spectra observed, and it is not intended to suggest in this work that the appearance of finite values for intensity at a point determined by the above energy levels constitutes an unambiguous identification of an observed level for CO_2^+. As an example, our data would not separate out the (2,0,0) components from those of components of the (1,0,1) and the (1,2,0) levels. The (1,2,0) level would be split into four levels by the Renner–Teller and spin–orbit interactions, the upper two of which are approximately coincident with the (2,0,0) levels. Furthermore, in our recent publication[6] including some electron spectra at higher resolution, members of the $(v_1,0,2)$ progression were clearly identified, but these could not be distinguished from some members of the progressions we have selected as a model for our fitting procedure. From the point of view of the fitting procedure the actual identification of the peaks found is not important.

To accomplish the fitting, relative peak positions were fixed by the spectroscopic model chosen, the peak widths were fixed as outlined in the previous discussion and the heights of the photoelectron peaks were allowed to vary to minimize the fitting errors using the method of least squares. After many trials it soon became evident which the most important vibrational modes were to achieve a reasonable fit, and this model, i.e., set of vibrational modes, was adopted as a basis for the analysis. At energies above ~2 eV from the threshold, it was not possible to resolve the individual vibrational peaks and they were often seen as a modulated background whose intensity was accounted for by high members of the above progressions. In the wavelength region 652.08 to 680.98 Å it was sufficient to use only the first three progressions shown above; in the region 689.7 to 713.9 Å it was necessary to use the first four progressions; in the remainder the complete set was used. The only exception to this was the use of levels of the type $(v_1,1,1)$ in the 689.77 to 694.64 Å region where this addition improved the fit somewhat but did not suggest itself elsewhere and hence will not be pursued in this report.

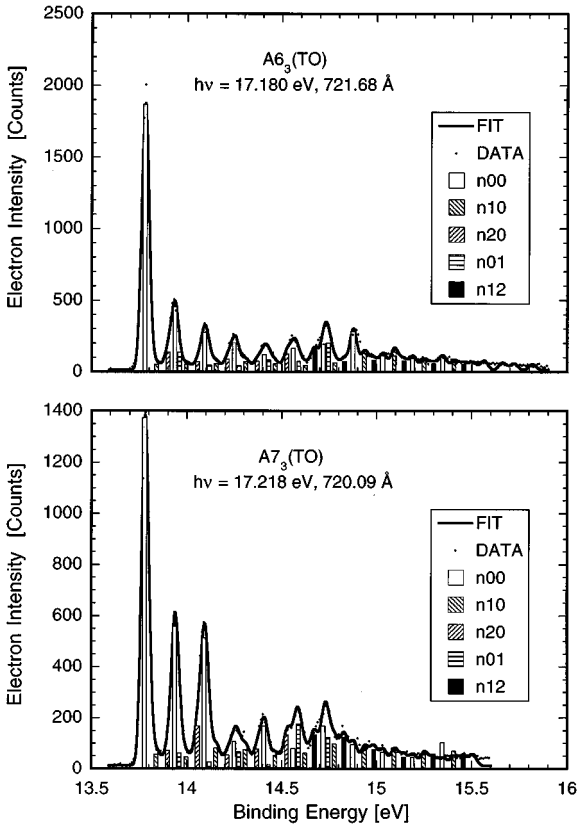

FIG. 1. Photoelectron spectra of CO_2 taken at the two resonant wavelengths shown, with the fitted curves and the vibrational members used in the fit. The spectrometer with angle was 0°. The solid line, FIT, is the calculated fit to the data points, DATA.

After fitting, each data set and the fit were inspected, and the model varied by adding or removing vibrational modes as required to achieve the best fit. Figure 1 shows the quality of the fit obtained by the 0° analyzer at photon energies of 17.180 and 17.218 eV. Both fits were accomplished using the same model for vibrational state composition, even though the structure is substantially different in these two closely spaced regions of the absorption spectrum. The vertical lines in the figures are the calculated amplitudes of the contributions from the progressions listed. The solid line, FIT represents the result of the calculated fit to the data points, DATA.

It can be seen that the data are of sufficient quality to give reliable intensities for the vibrational components marked, allowing vibrational branching ratios down to the 5% level to be measured. In the later figures the uncertainties shown include the statistical element (type *A* uncertainty[21]), derived from the fitting procedure, and further uncertainties from our measurements of the polarization of the incoming light and the calibration of the tungsten photodiodes (type *B* uncertainty). In general, the statistical error gave the largest contribution to the total uncertainty. The error bars shown on the data represent the combination in quadrature of the *A* and *B* type uncertainties, calculated with the appropriate error

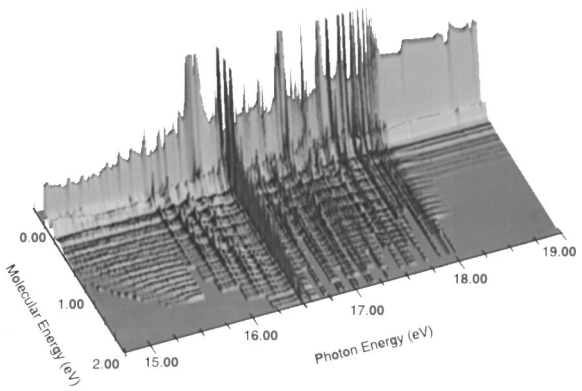

FIG. 2. A three dimensional plot of the electron spectra, corrected both for angular distribution effects and analyzer efficiencies. Molecular energy corresponds to the internal energy of the molecular ion, most of which is vibrational energy.

propagation procedures from the equations used to calculate the branching ratios and asymmetry parameter from the raw data.

Having obtained the intensities for the vibrational levels from each of the two analyzers, we then used these data, together with the measured light polarization, to calculate the β parameters and branching ratios. Figure 2 shows the β-independent electron spectra, calculated from the electron spectra taken at $\theta=0°$ and $\theta=90°$ which themselves have been corrected for the varying detection efficiency of the analyzers. The value of β can be deduced from the ratio of the electron intensity at $\theta=0°$ and $\theta=90°$ and the value of vibrationally resolve branching ratios calculated from the equation given earlier. The most intense peaks have been truncated, in order to reveal the detail in the higher vibrational modes.

As a check on the wavelength scale and the actual optical resolution obtained, we constructed a relative absorption cross section using the following procedure: All the electron counts at a particular wavelength for each analyzer were added. A β-independent value for the intensity was then obtained as outlined above, for each wavelength, the only further correction being for the varying tungsten photodiode response with wavelength. The result is shown in Fig. 3, and gives a result gratifyingly close to the photoionization spectrum measured by other authors.[5,22] The use to which we put this spectrum will be discussed further below.

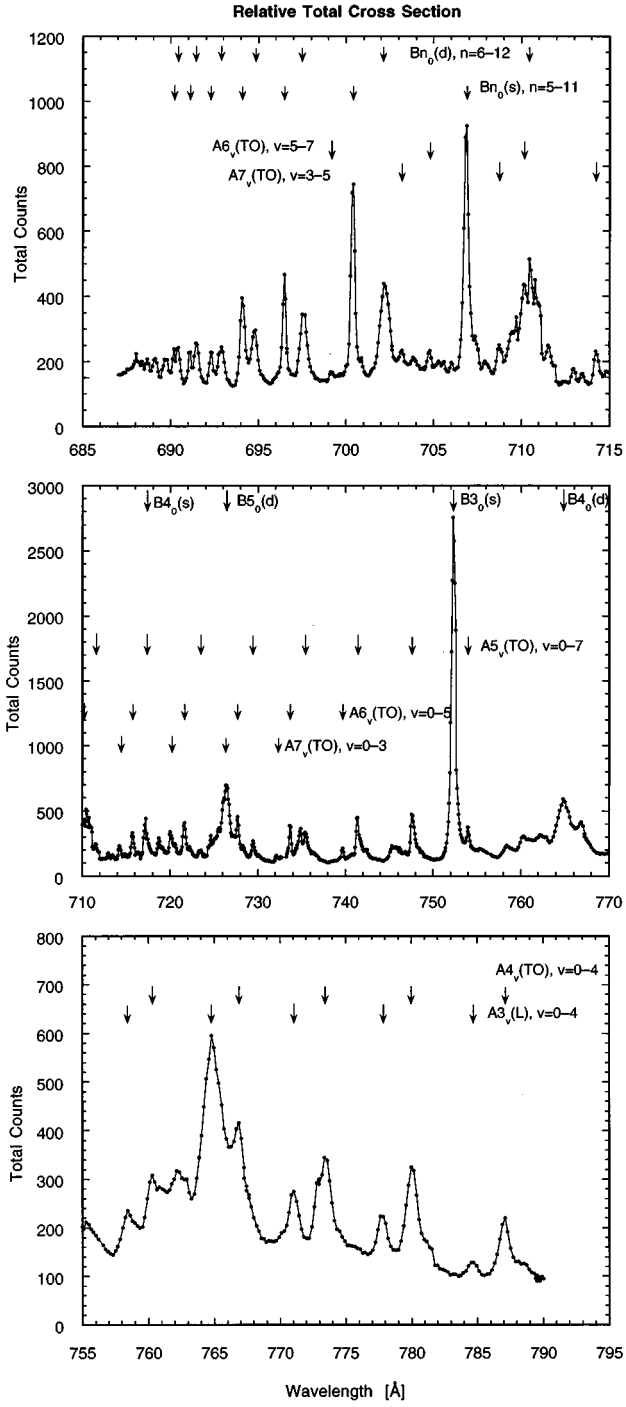

FIG. 3. The relative total cross section, calculated by integrating the electron spectra after correcting for angular distribution effects and electron analyzer efficiencies.

IV. DISCUSSION

With the large amount of data and the level of detail available to us here, in the first instance it seemed logical to concentrate in this paper on the response of the symmetric stretch vibrational members of the CO_2^+ ion to the series of resonances previously identified as the Henning sharp and diffuse series, the Tanaka–Ogawa series and the Lindholm series. For the purposes of convenience and brevity, we have followed the notation adopted by McCulloh[5] to label the series members; for example, $A5_2(TO)$ means the member of the Tanaka–Ogawa series for which the running principal quantum number is 5 and the vibrational quantum number is 2. Bearing in mind that this series is now believed to have $nd\delta_g$ symmetry, the principal quantum number should be 4, i.e., one less than shown on the graphs. In the case of the Henning series, though using McCulloh's notation, we follow the reassignment given by Fridh *et al.*,[23] and the running numbers shown are the principal quantum numbers. This results in our labeling of the resonances being different from that in McCulloh's table.

It will be seen from Fig. 3 and later figures that we have resolved most of the structure in Berkowitz's[22] photoionization yield spectrum, our optical resolution of 0.1 Å being not quite as good as his. There is an uncertainty, ~0.1 Å, in our absolute wavelength calibration, though we expect the relative positions of the absorption peaks seen in Fig. 3 to be correct within 0.01 Å. We then used our relative cross section data to identify the positions of the resonances on our wavelength scale. Having identified the wavelength of a particular resonance from the peak in the relative absorption cross section, we then used this wavelength to determine the values of the partial cross section and β parameter for that resonance. This procedure was important, because in many cases the peak of either β or the branching ratio appeared at a different wavelength from the absorption peak, as can happen in the region of a resonant structure which can decay into various different channels; this provided an internally consistent way of presenting this aspect of the results.

In Fig. 3 we have identified the most prominent series, but as can be seen much unidentified structure remains. In accordance with McCulloh's notation, the resonances labeled A converge to the $A\ ^2\Pi_u$ state of the ion, and those marked B to the $B\ ^2\Sigma_g^+$ state. As a first step in the analysis we show in Figs. 4–7 the vibrational branching ratios and β parameters for the eight members of the symmetric stretch vibrational progression in the CO_2^+ ion ground state, at the resonance positions of the various series. The lines joining the points on these figures are shown merely to guide the eye, and should not be regarded as any form of interpolation. This has been done for the first two vibrational members and occasionally the third member, but to avoid confusion this has not been done for the higher members since generally they lie close together, in fact overlapping within their error bars.

We make the following general observations, again with a note of caution because in some instances the spin–orbit split components of the antisymmetric stretch vibration overlap those of the symmetric stretch. We do not resolve either the spin–orbit or Renner–Teller splitting in our electron spectrum, so some of the effects seen for the higher vibrational members could be attributable to a mixture of these levels.

(1) The (000) and (100) members share most of the intensity, with the (000) member tending to dominate in the case of the two Henning series.
(2) There are strong variations in the relative strengths of the higher vibrational members, although some of these variations lie within experimental error.
(3) The β parameters lie in the range $0.5 \rightarrow -0.5$, with a tendency for the (000) and (100) members to lie at the lower end of this range.
(4) Rarely does the branching ratio of the most intense member, usually (000), rise above 0.5.
(5) Where there is a large scatter in the β parameters, this often occurs in regions of overlapping structure.

There are some notable exceptions to the above observations which will be reviewed according to spectroscopic series identification.

A. Tanaka–Ogawa series

Shown in Figs. 4 and 5 are the results of the analysis for the TO series. In general we have sufficient optical resolution to resolve the spin–orbit split members of these series, but since the $^2\Pi_{1/2}$ components, at the shorter wavelength of the pair, are expected to have the larger intensities, these are the ones we identify on our spectra. Where ambiguities arise we have done an interval analysis, using the fact that the vibrational progressions should have an approximately constant energy separation of 139 meV. In some cases there is disagreement with McCulloh's wavelength values for the resonance position. For example, he gives 735.2 and 734.7 Å for the spin–orbit split components of the $A5_3$ resonance, whereas we are using 735.38 Å for the $^2\Pi_{1/2}$ component. Our values for the other resonance positions are consistent with the published values within our wavelength error of ~0.1 Å, so in this particular case we suggest that the $^2\Pi_{3/2}$ component is the weak feature at 736.24 Å on our wavelength scale.

The $A4_3$ resonance has a high (000) branching ratio and stands out from the other vibrational members; its β parameter is the lowest for this series at around -0.7. Also [hidden by the symbol for (100) the (700)] branching ratio has the same value as the (100).

The $A5_4$ resonance shows the largest variation in β, with a low value, -0.7, for the (000), and a high value, 0.8, for the (500) member. The $A5_2$ resonance exhibits similar behavior.

The $A6_5$ and $A6_7$ resonances stand out from the other resonances in this progression, with high values for their branching ratios. The β parameters show somewhat different behavior, with the values for the $A6_7$ resonance ranging from $-0.5 \rightarrow 0.8$, and those for $A6_5$ covering a much smaller range, but the values for the (000) member are in line with the general behavior for this vibrational component with β around -0.5.

The $A7_v$ ($v=0$–5) vibrational progression shows no behavior markedly different from the general pattern; it is interesting perhaps to note that the (000) branching ratio varies in a smooth way as we proceed along the resonances, with a minimum value of 0.26 for the $A7_2$ member which is somewhat lower than the general value for this branching ratio.

B. Henning series

To avoid congestion among the higher series members, the data for the Henning series, have been plotted as numbered resonances in Figs. 6 and 7 (left), and there are some qualitative differences between their behavior and those of the resonances converging to the A state of the ion. The values of the internuclear distance are similar for the X and B states of the ion, so long vibrational progressions are not seen in contrast to the series converging to the A state. Most of the intensity is therefore expected in the (000) branching ratio for both series. With the exception of the $B5_0(d)$ resonance, the (000) branching ratios in the Henning diffuse series are above 0.5, particularly for the higher series members, in contrast with the Tanaka–Ogawa and Lindholm series where this ratio lies below 0.5. In the case of the sharp series

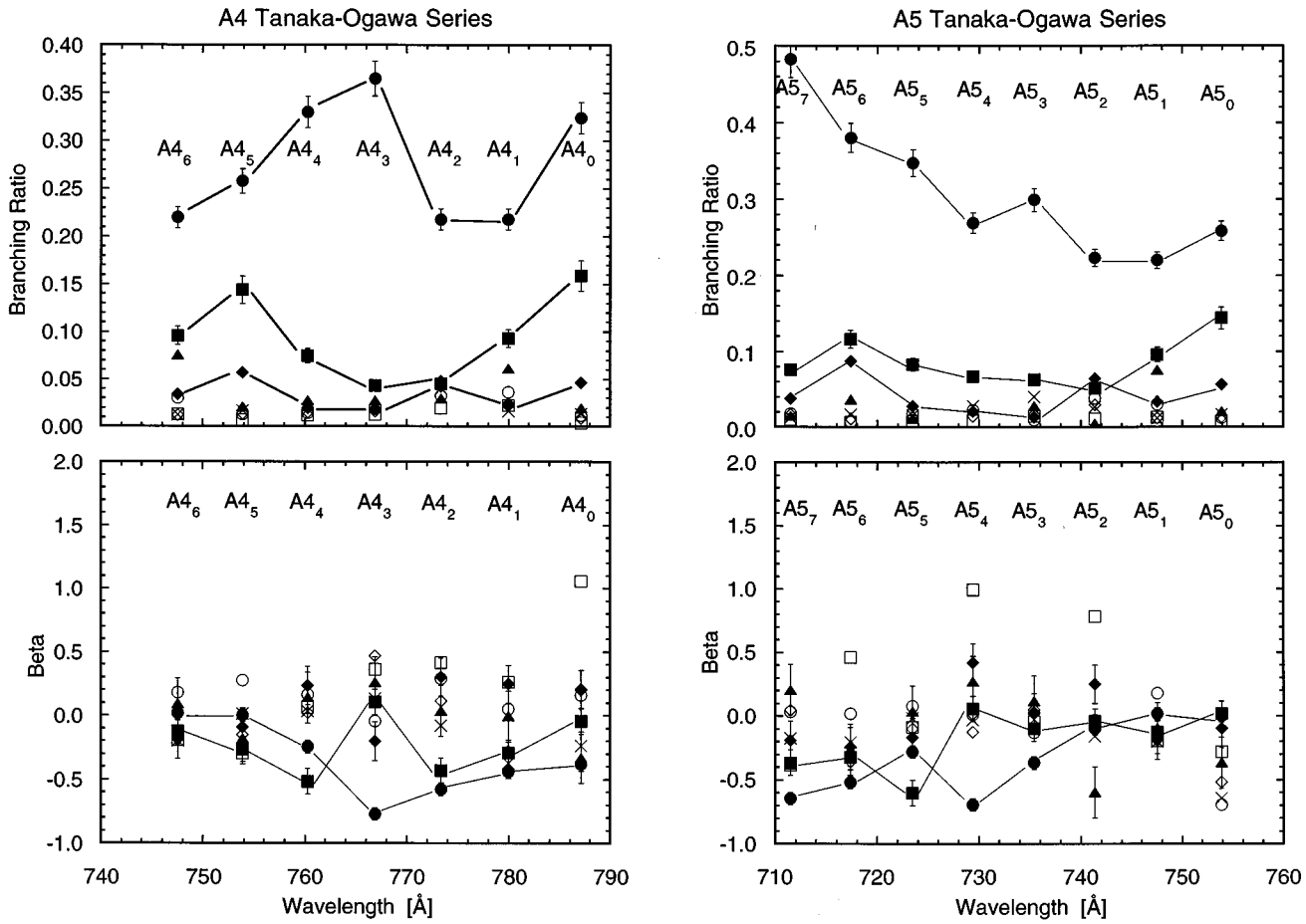

FIG. 4. Vibrational branching ratios for the ground state of the CO_2^+ ion, and β parameters, at the positions of the $A4$ and $A5$ Tanaka–Ogawa series members; ●, (000); ■, (100); ♦, (200); ▲, (300); ○, (400); □, (500); ◇, (600); ×, (700).

such a contrast is not evident, though there is perhaps a tendency towards higher branching ratios than is generally the case for the other series, with maxima around the $B5_0(s)$ and $B10_0(s)$ resonances. For both these series the β parameters are spread over a larger range, with particularly high values, around 1.5, for the (600) vibrational member at the $B8_0(d)$ and $B12_0(d)$ resonance positions, but as will be seen later this may be just a function of the peak shape. On the left of Fig. 7 values are given for the higher series members, where the sharp and diffuse lines are not separated within our experimental resolution. They exhibit broadly similar behavior to the other Henning series members.

One feature in some of the above exceptions to the ''general rule'' is that they occur where the resonance concerned overlaps more prominent structure, particularly Henning series members. The $A4_3(TO)$ and $A3_3(L)$ resonances lie on the wing and on top respectively of the $B3_0(s)$ resonance. The $A5_4(TO)$ resonance lies on the wing of the $B5_0(d)$ peak, and the $A6_5(TO)$ resonance overlaps the $B6_0(d)$. The $A6_7(TO)$ resonance lies in the wing of the $B7_0(d)$, and it is perhaps noteworthy that in the case of the $A7_v(TO)$ progression, whose members apart from $A7_4(TO)$ lie clear of other major resonant structures, the β parameters and branching ratios conform more or less to the general pattern. This explanation is not always reliable; note that, as well as the $A6_5(TO)$ resonance, the $A5_7(TO)$, and $A7_4(TO)$ resonances also lie in the wings of the $B6_0(d)$ resonance, making this a rather complex structure, and the $A6_2(TO)$ lies on the wing of the $B5_0(d)$. Yet these resonances fit more or less the general pattern.

C. Lindholm series

Figure 7 (right) show the results of the Lindholm series. The $A3_2$ and $A3_3$ members of the two series visible in our spectra stand out, the first with a positive value for β around 0.7 for the (300) vibrational member and thus the highest for this set. More striking is the high branching ratio for (000) member at the $A3_3$ resonance, well above the values for the other resonances; the branching ratios for the other vibrational members at this resonance all lie together below 0.06.

V. SPECTRAL RESPONSE OF BRANCHING RATIOS AND β PARAMETERS

It is perhaps more instructive to examine continuous plots of the β parameter and branching ratios, and for this purpose Figs. 8–16 were constructed. Immediately in Fig. 8 the different response of the (000) branching ratio to the

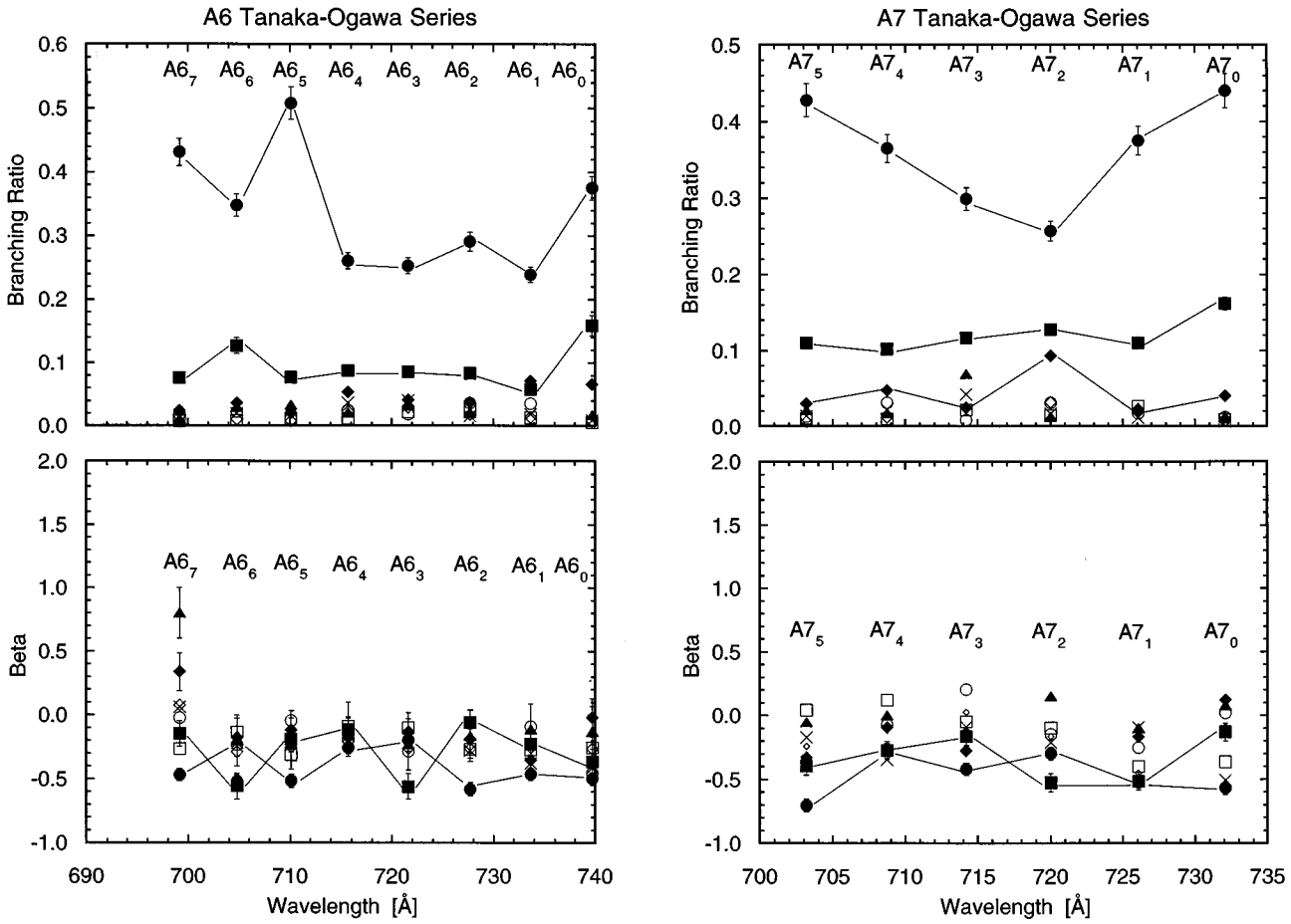

FIG. 5. Vibrational branching ratios for the ground state of the CO_2^+ ion, and β-parameters, at the positions of the $A6$ and $A7$ Tanaka–Ogawa series members; ●, (000); ■, (100); ♦, (200); ▲, (300); ○, (400); □, (500); ◇, (600); ×, (700).

sharp and diffuse Henning series is apparent, with dips corresponding to the sharp series and peaks to the diffuse. The behavior of the β parameter is rather striking, showing a rather fine series of repetitive structures whose shapes are reminiscent of the structure predicted[24] and measured[25] some while ago for the $5p$ β parameter in the region of the autoionizing lines between the $^2P_{1/2\ 3/2}$ limits in xenon. It seems this comparison cannot be carried much further, for xenon, the ns series was predicted to show sharp peaks in the β parameter, which in fact were not seen in the experiment. Although such peaks are seen quite clearly here, they occur for the sharp series with its different symmetry $nd\sigma_g$. Note that the positions of the diffuse series lie on the falling edges of these structures, and that this repetitive pattern is undisturbed by other structure until we reach the $B4_0(s)$ and $B5_0(d)$ resonances. Presumably at this point the ''pairs'' of resonances are now too far apart to interact substantially, and also the rich structure converging to the A state threshold at 716.1 Å begins to dominate. In Fig. 9 we see the $A5_v(TO)$ and $A6_v(TO)$ series clearly resolved as dips in the branching ratios, and asymmetric profiles standing out clearly in the β parameters for the $A5_1$ and $A5_2$ members.

At longer wavelengths, shown in Fig. 10, the $A3$ Lindholm and $A4$ Tanaka–Ogawa series lie close together, producing another set of repetitive structures. The Lindholm series is responsible for dips in the β values, while the Tanaka–Ogawa correlates with peaks. Both series produce dips in the (000) branching ratio until this pattern is disturbed by the most intense resonance in the whole spectrum, the $B3_0(s)$. This behavior of the β parameters indicates different symmetries for the two series; Lindholm[3] originally put forward nd symmetry for his series, since the TO series are now thought to be $(1\pi_u)^{-1}nd\delta_g\,^1\Pi_u$, one option for his series is $(1\pi_u)^{-1}nd\pi_g\,^1\Sigma_u^+$.

It is clear that in the resonance regions intensity is being taken from the (000) vibrational member and distributed among the other members. From Figs. 4–7 we can see that not all of this intensity goes into the symmetric stretch vibrational progression; by adding the branching ratios at a particular resonance it is apparent that substantial intensity is going into the bending and asymmetric stretch modes, well over 50% in some cases (see Table I).

Generally the individual branching ratios for these other modes are less than 0.1, but even so the data are of sufficient quality for the resonant structures to be seen clearly. We show a sample of our data for the (010) and (110) bending modes that are normally forbidden in Figs. 11 and 12. The β parameters are generally negative, around -0.5, and their

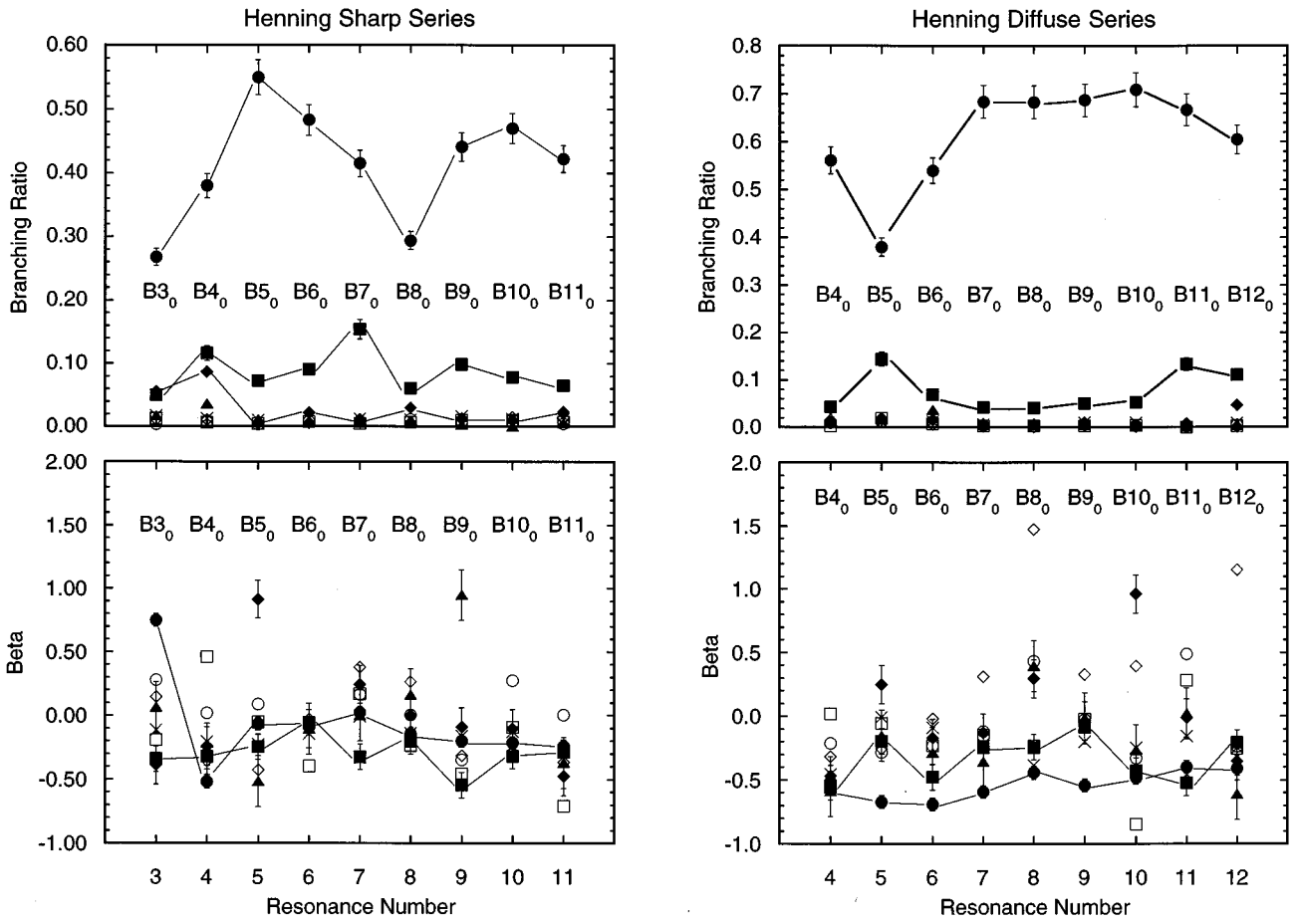

FIG. 6. Vibrational branching ratios for the ground state of the CO_2^+ ion, and β parameters, at the positions of the Henning sharp and diffuse series members; ●, (000); ■, (100); ◆, (200); ▲, (300); ○, (400); □, (500); ◇, (600); ×, (700). To avoid congestion in the figure, the resonances have not been plotted on a wavelength scale.

response to the series converging onto the A state is rather less pronounced than that of the branching ratio. We also found that they did not respond strongly to the Henning sharp and diffuse series in the region where they overlap. Most of the TO series members can be clearly identified in the branching ratio spectra, usually as a dip in the branching ratio. A similar picture emerges for the (110) data, where the branching ratios show the resonant structure most prominently. It is worth noting that this behavior, i.e., minima in the branching ratios, is consistent with our earlier finding from a high resolution measurement,[6] that at the $A5_2$ resonance no contribution to these normally forbidden odd quanta bending modes could be clearly identified. It can be seen from Figs. 11 and 12 that this is in contrast to the behavior of the branching ratios in the region of the Henning series members. Again, some caution is needed because of the unresolved components in our electron spectra, but our fitting procedure gives us some confidence that these bending modes are populated.

Although ionization to the (000) vibrational level of the CO_2^+ ion represents less than half of the cross section, by separating out this contribution a clearer picture of the resonant structures can emerge. Thus more detail is identifiable from the (000) branching ratio than from the absorption spectrum. We have calculated the expected wavelengths for the higher members of the vibrational progressions corresponding to the $A3$ Tanaka–Ogawa and $A4$ Lindholm series, and have identified the $A3_5$ and $A3_6$ members at 751.86 and 745.57 Å, and the $A4_3$ and $A4_4$ members at 734.55 and 728.55 Å, on our wavelength scale. Some higher Rydberg members of the Lindholm series, $A5_0$ (739.1 Å), $A6_0$ (731.7 Å), and $A7_0$ (727.4 Å) converging to the $A\ ^2\Pi_{u,1/2}$ state of the ion, can possibly also be seen, but no positive identification can be made because they are overlapped by the members of the TO series converging to the $A\ ^2\Pi_{u,3/2}$ state of the ion.

In an initial approach to theoretical analysis of the branching ratio data, we have calculated the Franck–Condon factors using the method outlined by Sharp and Rosenstock[26] for polyatomic molecules. The vibrational wave functions were expressed as a product of Hermite polynomials, and using the method of generating functions a power series expansion was created whose coefficients were the intensities of the vibrational modes of the molecule. For resonances

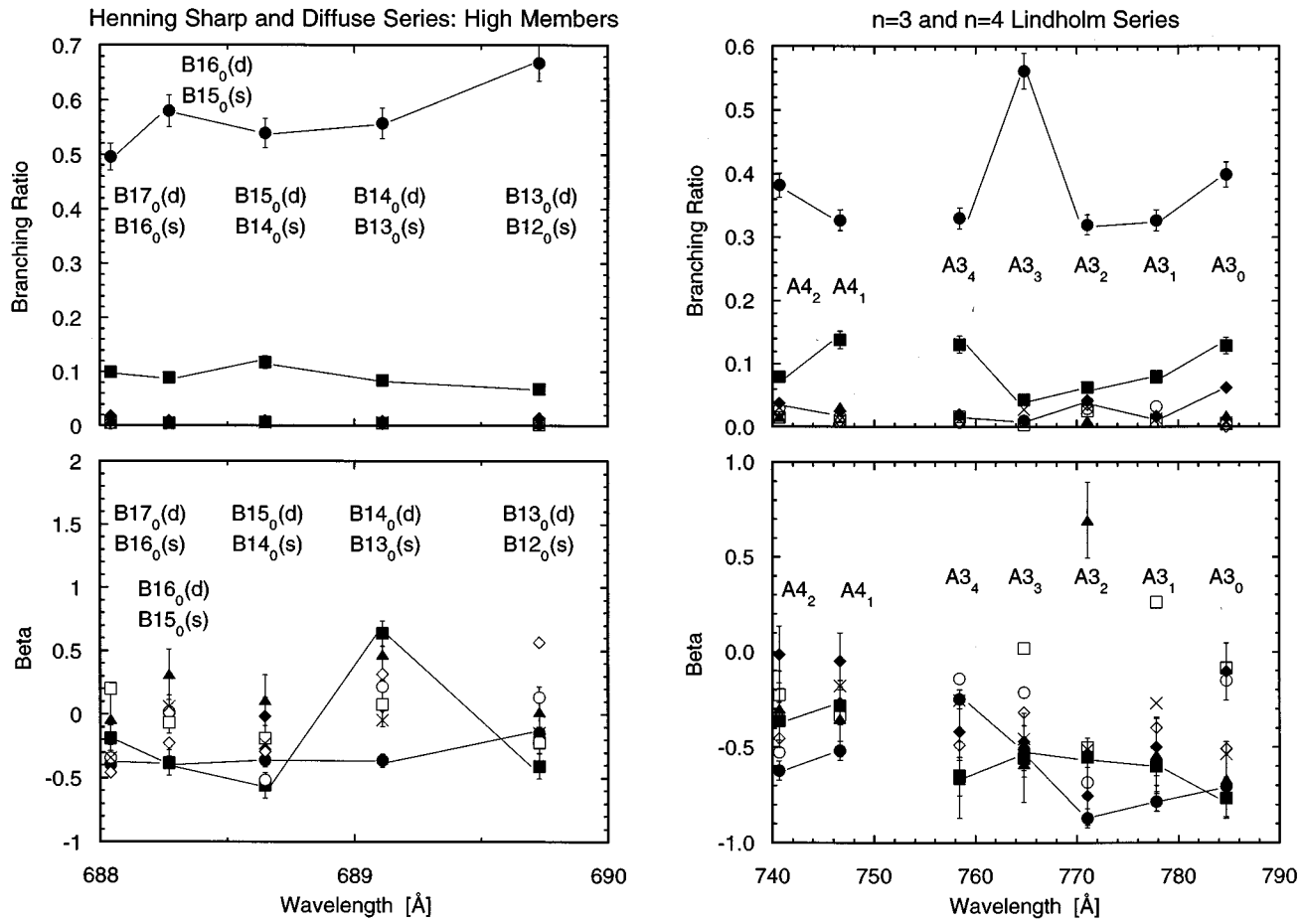

FIG. 7. Vibrational branching ratios for the ground state of the CO_2^+ ion, and β parameters, at the positions of the unresolved members of the Henning sharp and diffuse series members, and for the $A3$ and $A4$ Lindholm series members; ●, (000); ■, (100); ◆, (200); ▲, (300); ○, (400); □, (500); ◇, (600); ×, (700).

converging to the A state of the ion it was assumed that their molecular constants would be the same as those for the ion and were taken from Gauyacq *et al.*;[27] the transition probabilities to the ion vibrational levels were then calculated and compared to the experimental values in Table I. A similar procedure was used for the Henning series, where the B state molecular constants were taken from Gauyacq *et al.*[28] The theoretical calculation is normalized such that the sum of all the vibrational intensities resulting from the decay of a particular resonance by autoionization is equal to one; the experiment, however, is a little different from this, because it measures relative intensities at the resonant wavelength, and this can of course include a nonresonant contribution. This has to be borne in mind when making comparisons between the theoretical values in Table I and the experimental ones. If the Franck–Condon principle is upheld then it could be assumed that the theoretical value will lie between the resonant and off-resonant values, and also that as one proceeds up a Rydberg progression the agreement between experiment and theory should improve, since the approximation of using the molecular constants for the ion state to which the resonances converge improves. It can be seen from the table that the above assumptions are not in general valid, except for the $A4_1$ series ionizing to the ion (000) vibrational level, where the branching ratios do approach the theoretical value. There are other cases where the agreement is approximate, but for many of the transitions observed in the experiment the theoretical intensities are very small, and zero for the forbidden transitions to the odd numbered overtones. As seen in Table I, this results in the sum of the experimental values at a particular resonance being less than unity, because, as stated earlier, a sizeable fraction of the intensity goes into the other vibrational modes. In contrast, the sum of the theoretical values shown is close to unity since there is almost no intensity outside the main vibrational progression.

VI. CONCLUSIONS

It can be seen from the above that, in the regions where individual series can be identified clearly without complication from overlapping structure, the β parameters and branching ratios show distinctive behavior which can be associated with that series. Examples of this are the Henning series and Tanaka–Ogawa and Lindholm series, and even where these series overlap each other, quite distinctive structures in the β parameter are seen. As soon as there is the

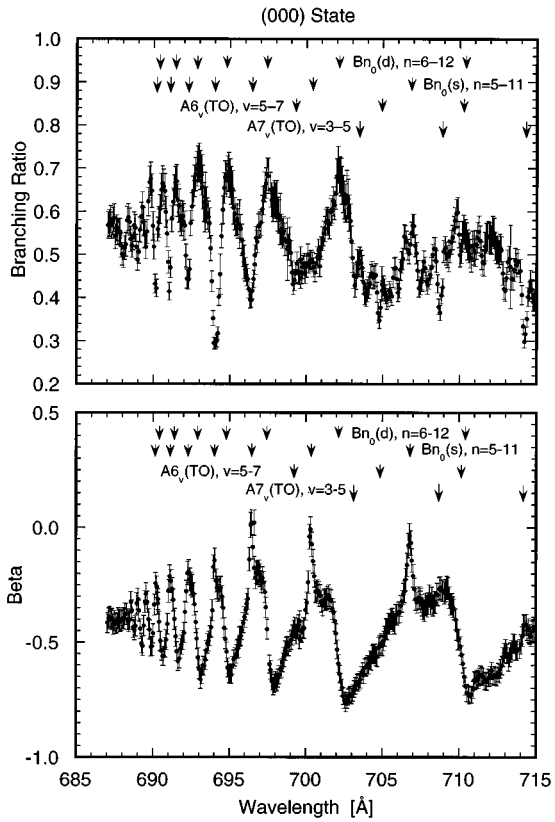

FIG. 8. Branching ratios and β parameters for the (000) vibrational level of the ground state of the CO_2^+ ion, in the wavelength region where the Henning series are prominent.

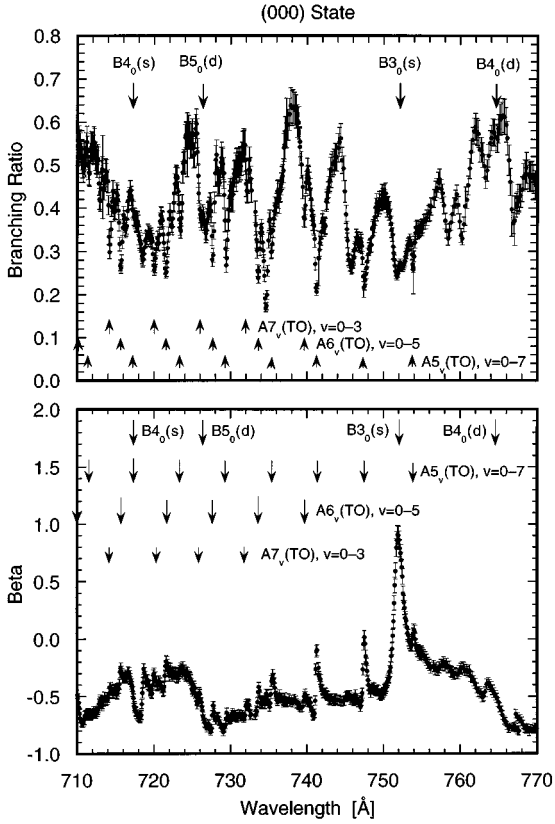

FIG. 9. Branching ratios and β parameters for the (000) vibrational level of the ground state of the CO_2^+ ion, in the wavelength region where the Tanaka–Ogawa series are prominent.

possibility of multiple interactions between series members, it is difficult to discern any specific behavior for a particular series. The general rules, as outlined above, indicate that β lies between 0 and -0.5, and more often than not the β parameter goes up in the resonant regions, the most noticeable exception being the Lindholm series. This is similar to the finding in our recent higher resolution experiment in which the ion's X state spin–orbit splitting was resolved,[6] and is counterintuitive in one respect since at the resonance angular momentum exchange between the ionized electron and the core can lead to parity unfavored transitions, and thus negative values of β are expected. We note, however, that if the resonance peak position is defined from the absorption spectrum, as we described above, then the peaks in the β parameter do not always coincide with this, and can in fact be on either side of it. This behavior was noted by Hu[29] in a preliminary analysis of this data set, and this is why the β values for the resonance position are different from the peak value and often negative, as seen in Figs. 4–7. This demonstrates that a theoretical calculation is required of the response of β and the branching ratio over the width of the resonant line, before any conclusions can be drawn concerning the autoionization dynamics. This should be practical in regions where particular series dominate, but elsewhere, at our level of resolution, would appear to be unrealistic.

The rather poor agreement between the calculations and the experimental data in the resonance regions is an indication that the Born–Oppenheimer approximation is not valid. Our calculations ignore the continuum contribution underlying the resonances, but even so one might at first expect that the experimental Franck–Condon factors would then lie between the resonance and off resonance values. It can be seen that this is generally not the case, and to use the method outlined by Smith[30] for O_2, where the profile of the autoionizing line is analyzed and the Franck–Condon factors calculated by taking into account both the continuum and autoionizing contributions, does not look promising for CO_2. Judging from the absorption spectrum, the background contribution does not appear to be particularly large, but nevertheless it may have the effect of frustrating analysis of these spectra in terms of a single partial wave picture, as was seen for the β parameter measurement for the $A5_2$ resonance.[6] Furthermore, the complexity of the CO_2 spectrum presents further difficulties in the analysis; it has been pointed out earlier that the peak or minimum of the branching ratio may not coincide with the resonance peak position identified from our relative cross section data, so the actual value shown in the table depends critically on the peak shape, and this in turn can depend on the shape and position of underlying or adjacent resonances.

The disagreement between our experiment and the Franck–Condon calculations, therefore, may be due to a

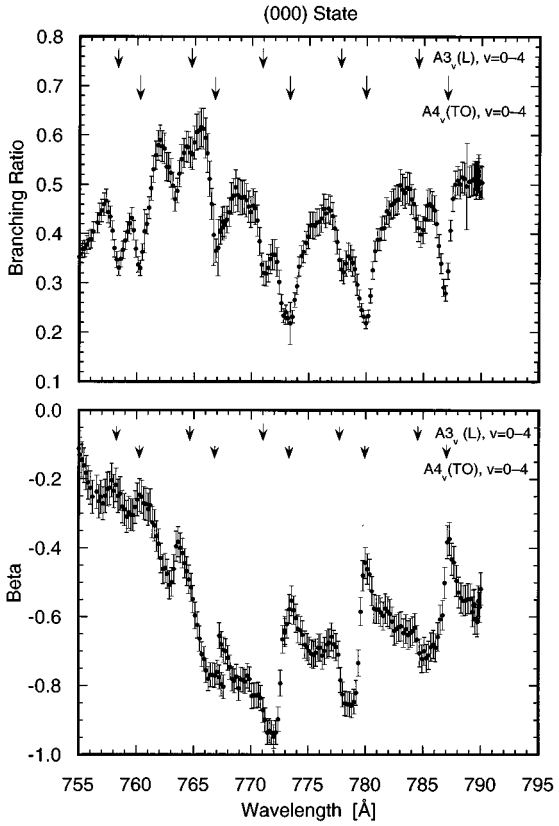

FIG. 10. Branching ratios and β parameters for the (000) vibrational level of the ground state of the CO_2^+ ion, in the wavelength region where the $A3$ Lindholm and $A4$ Tanaka–Ogawa series are prominent.

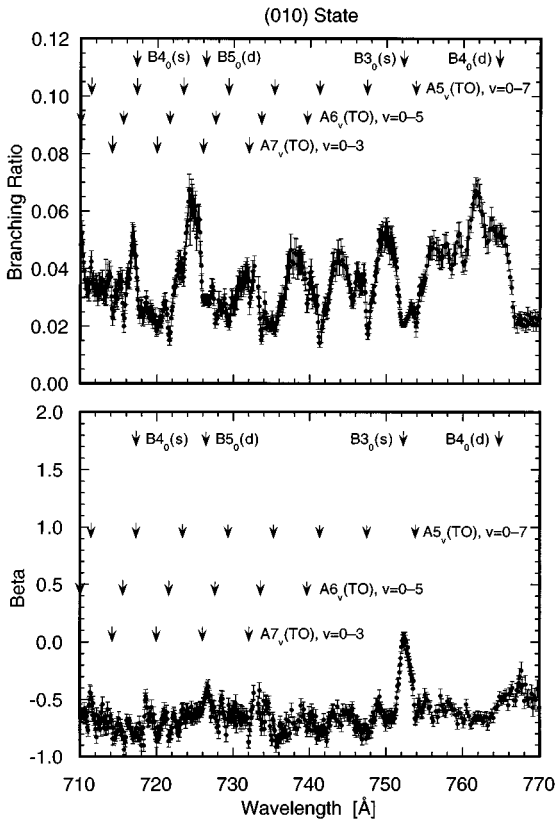

FIG. 11. Branching ratios and β parameters for the (010) vibrational level of the ground state of the CO_2^- ion, in the wavelength region where the Tanaka–Ogawa series are prominent.

TABLE I. The CO_2^+ ion ground vibrational branching ratios for the Tanaka–Ogawa Rydberg series members, and background values, for different vibrational quantum numbers. Theoretical values are shown for comparison.

Resonance	Wavelength	0	100	200	300	400	500	600	700	total
A40	787.11	0.3240	0.1590	0.0460	0.0193	0.0121	0.004 20	0.008 60	0.013 40	0.586 60
A50	753.89	0.2580	0.1440	0.0568	0.0209	0.0128	0.007 40	0.013 30	0.016 50	0.529 70
A60	739.68	0.4830	0.0760	0.0377	0.0152	0.0181	0.010 00	0.016 50	0.012 70	0.669 20
A70	732.08	0.4400	0.1620	0.0401	0.0124	0.0118	0.009 30	0.006 60	0.006 30	0.688 50
Theory		0.2230	0.3190	0.2430	0.1310	0.0557	0.020 50	0.006 50	0.001 80	1.000 00
A41	779.98	0.2180	0.0930	0.0219	0.0609	0.0362	0.022 10	0.024 00	0.016 10	0.492 20
A51	747.53	0.2200	0.0959	0.0338	0.0756	0.0300	0.013 10	0.012 10	0.012 30	0.492 80
A61	733.64	0.2390	0.0576	0.0713	0.0709	0.0353	0.012 70	0.013 80	0.018 40	0.519 00
A71	726.08	0.3750	0.1100	0.0226	0.0251	0.0173	0.026 40	0.022 30	0.011 60	0.610 30
Theory		0.3610	0.0570	0.0320	0.1620	0.2280	0.128 00	0.032 00	0.000 00	1.000 00
A42	773.36	0.2180	0.0930	0.0219	0.0609	0.0362	0.022 10	0.024 00	0.016 10	0.492 20
A52	741.36	0.2230	0.0511	0.0642	0.0050	0.0384	0.011 50	0.029 60	0.026 70	0.449 50
A62	727.7	0.2910	0.0835	0.0372	0.0198	0.0361	0.025 20	0.018 10	0.015 70	0.526 60
A72	720.01	0.2570	0.1280	0.0933	0.0132	0.0314	0.014 40	0.032 20	0.016 50	0.586 00
Theory		0.2830	0.0586	0.1860	0.0208	0.0342	0.139 00	0.164 00	0.115 00	1.000 00
A43	766.86	0.3650	0.0431	0.0187	0.0272	0.0214	0.013 10	0.016 30	0.043 20	0.548 00
A53	735.38	0.2990	0.0632	0.0134	0.0276	0.0097	0.014 50	0.016 50	0.039 90	0.483 80
A63	721.6	0.2530	0.0862	0.0413	0.0320	0.0189	0.022 40	0.029 10	0.040 10	0.523 00
A73	714.2	0.2990	0.1170	0.0251	0.0694	0.0083	0.021 90	0.024 50	0.042 30	0.607 50
Theory		0.1800	0.3300	0.0170	0.0700	0.1500	0.003 30	0.070 00	0.180 00	1.000 00
Theory	Background	0.8670	0.1120	0.0210	0.0000	0.0000	0.000 00	0.000 00	0.000 00	1.000 00
Experiment	Background 783	0.4980	0.0761	0.0336	0.0122	0.0120	0.006 40	0.009 60	0.011 80	0.659 70
Experiment	Background 750	0.4290	0.1060	0.0313	0.0145	0.0087	0.003 80	0.007 90	0.010 50	0.611 70

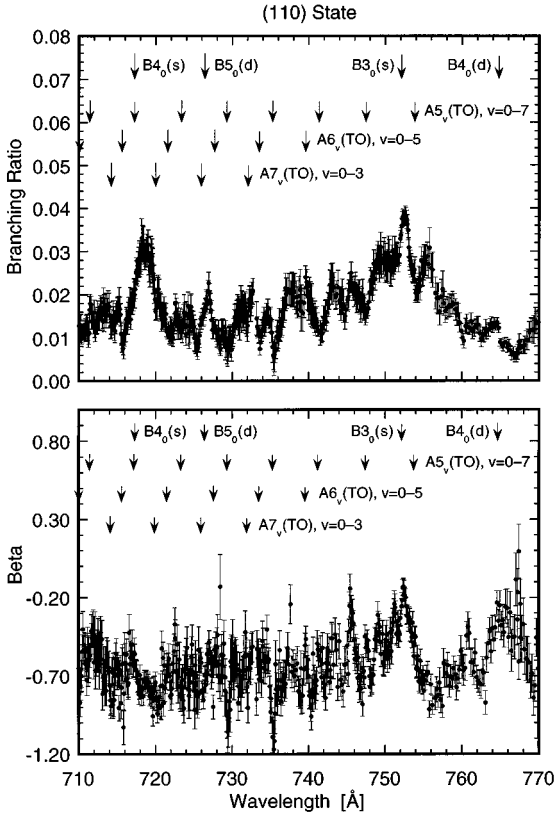

FIG. 12. Branching ratios and β parameters for the (110) vibrational level of the ground state of the CO_2^+ ion, in the wavelength region where the Tanaka–Ogawa series are prominent.

combination of causes. For example, the calculations do not include the effects of vibronic coupling, and, in view of the complex structure, it seems unlikely that a calculation including such coupling is feasible for this molecule in this spectral region. Cederbaum[31] has calculated the effects of vibronic coupling where the number of interacting electronic states is not large and where there is one vibrational degree of freedom, but points out that the complexity increases enormously if additional vibrational modes are present. Since our experiment shows that a considerable fraction of the intensity goes into vibrational modes other than the fundamental symmetric stretch, it is clearly going to be important to include vibronic coupling in any theoretical analysis of these data. In spite of the above, there are some areas where a theoretical calculation could be instructive. The periodic structures seen for β in Fig. 8 are clearly caused by the interaction between members of the Henning sharp and diffuse series, and are not seriously affected by other series. Similarly the β parameters for the $A4(\mathrm{TO})$ and $A3(L)$ series in Fig. 10 show distinctive behavior and are well separated from other structure. Also, the combination of both branching ratio and β-parameter data can be useful in further analysis and assignment of the resonant structure. We have concentrated in this paper on the general features of the behavior of the most intense of the vibrational components; in a future publication, and as the next step in the analysis of this data set, we shall examine in more detail the behavior of the weaker vibrational modes.

ACKNOWLEDGMENTS

We are grateful for financial support from the Engineering and Physical Sciences Research Council, UK, and the U.S. Department of Energy, Office of Energy Research under Contract No. W-31-109-ENG-38.

[1] Y. Tanaka and M. Ogawa, Can. J. Phys. **40**, 879 (1962).
[2] Y. Tanaka, A. S. Jursa, and F. J. LeBlanc, J. Chem. Phys. **32**, 1199 (1960).
[3] E. Lindholm, Ark. Fys. **40**, 129 (1969).
[4] H. J. Henning, Ann. Phys. (Leipzig) **13**, 599 (1932).
[5] K. E. McCulloh, J. Chem. Phys. **59**, 4250 (1973).
[6] A. C. Parr, P. M. Dehmer, J. L. Dehmer, K. Ueda, J. B. West, M. R. F. Siggel, and M. A. Hayes, J. Chem. Phys. **100**, 8768 (1994).
[7] N. Padial, G. Csanak, B. V. McCoy, and P. W. Langhoff, Phys. Rev. A **23**, 218 (1981).
[8] P. M. Dittman, D. Dill, and J. L. Dehmer, Chem. Phys. **78**, 405 (1983).
[9] D. M. P. Holland, J. B. West, and M. A. Hayes, Chem. Phys. **148**, 241 (1990).
[10] A. C. Parr, D. L. Ederer, J. L. Dehmer, and D. M. P. Holland, J. Chem. Phys. **77**, 111 (1982).
[11] D. M. P. Holland, J. B. West, A. A. MacDowell, I. H. Munro, and A. G. Beckett, Nucl. Instr. Meth. B **44**, 233 (1989).
[12] A. C. Parr, S. H. Southworth, J. L. Dehmer, and D. M. P. Holland, Nucl. Instr. Meth. **222**, 221 (1984).
[13] G. V. Marr and J. B. West, At. Data and Nucl. Data Tables **18**, 497 (1976).
[14] D. M. P. Holland, A. C. Parr, D. L. Ederer, J. L. Dehmer, and J. B. West, Nucl. Instr. Meth. **195**, 331 (1982).
[15] J. B. West, *Vacuum Ultraviolet Photoionization and Photodissociation of Molecules and Clusters*, edited by C.-Y. Ng (World Scientific, Singapore, 1991), Chap. 8.
[16] R. Stockbauer, B. E. Cole, D. L. Ederer, J. B. West, A. C. Parr, and J. L. Dehmer, Phys. Rev. Lett. **43**, 757 (1979).
[17] H. Veenhuizen, B. Wannberg, L. Mattsson, K. E. Norell, C. Nohre, L. Karlsson, and K. Siegbahn, J. Elec. Spectrosc. Relat. Phenom. **41**, 205 (1986).
[18] D. Gauyacq, C. Larcher, and J. Rostas, Can. J. Phys. **57**, 1634 (1979).
[19] L.-S. Wang, J. Reutt, Y. T. Lee, and D. A. Shirley, J. Elec. Spectrosc. Relat. Phenom. **47**, 167 (1988).
[20] G. Chambaud, W. Gabriel, P. Rosmus, and J. Rostas, J. Phys. Chem. **96**, 3285 (1992).
[21] B. Taylor and C. Kuyatt, *Guidelines for Evaluating and Expressing the Uncertainty of NIST Measurement Results*, Natl. Inst. Stand. Tech. Note 1297, 2nd ed. (GPO, Washington, D.C., 1994).
[22] J. Berkowitz, *Photoabsorption, Photoionization and Photoelectron Spectroscopy* (Academic, New York, 1979).
[23] C. Fridh, L. Åsbrink, and E. Lindholm, Chem. Phys. **27**, 169 (1978).
[24] D. Dill, Phys. Rev. A **7**, 1976 (1973).
[25] J. A. R. Samson and J. L. Gardner, Phys. Rev. Lett. **31**, 1327 (1973).
[26] T. E. Sharp and H. M. Rosenstock, J. Chem. Phys. **41**, 3452 (1964).
[27] D. Gauyacq, C. Larcher, and J. Rostas, Can. J. Phys. **57**, 1959 (1979).
[28] D. Gauyacq, M. Horani, S. Leach, and J. Rostas, Can. J. Phys. **53**, 2040 (1975).
[29] X.-M. Hu, Ph.D. thesis, University of Aberdeen, UK, 1990.
[30] A. L. Smith, J. Quantum Spectrosc. Radiat. Transfer **10**, 1129 (1970).
[31] L. S. Cederbaum, J. Chem. Phys. **78**, 5714 (1983).